C.P. No. 187
(16,887)
A R C Technical Report

MINISTRY OF SUPPLY

AERONAUTICAL RESEARCH COUNCIL

CURRENT PAPERS

Compressor Cascade Flutter Tests

20° Camber Blades, Medium and High Stagger Cascades

By

D. A. Kilpatrick and J. Ritchie

LONDON · HER MAJESTY'S STATIONERY OFFICE

1955

Price 2s 6d net

C.P. No. 187
Report No. P. 133
December, 1953.

NATIONAL GAS TURBINE ESTABLISHMENT

Compressor Cascade Flutter Tests

20° Camber Blades, Medium and High Stagger Cascades

- by -

D. A. Kilpatrick and J. Ritchie

SUMMARY

The tests reported show the existence of three main zones of flutter at high stress; stalling flutter, shock-stalling flutter and choking flutter. These zones are similarly located (with reference to the aerodynamic characteristics) for both the medium and the high stagger cascades tested, and they extend over a wide range of incidence. Good correlation between the zones of flutter and the experimentally measured blade force derivatives, with respect to Mach number and incidence, has been obtained. More experimental data are, however, required before a quantitative analysis of the problem can be achieved.

		Page
1.0	Introduction	3
2.0	Description of Tests	3
	2.1 Cascade details	3
	2.2 Test techniques	3
3.0	Test results	4
	3.1 Medium stagger cascade	4
	3.1.1 Blade stresses	4
	3.1.2 Aerodynamic forces	5
	3.2 High stagger cascade	6
	3.2.1 Blade stresses	6
	3.2.2 Aerodynamic forces	6
4.0	Theoretical aspects	7
5.0	Discussion of results	8
6.0	Conclusions	9
	References	10

ILLUSTRATIONS

Fig. No.	Title
1	Cascade and tunnel arrangements
2	Nodal Pattern and Flutter Records
3	Flutter Characteristics for Medium Stagger Cascade
4	Location of Flutter (Medium Stagger Cascade)
5	Force Characteristics for Medium Stagger Cascade Blade
6	Comparison of Regions of Negative Slope Force Curves and Flutter
7	Flutter Characteristics for High Stagger Cascade
8	Location of Flutter (High Stagger Cascade)
9	Force Characteristics for High Stagger Cascade Blade

1.0 Introduction

The axial-flow compressor blade flutter problem, which has existed for a number of years, has more recently become increasingly prominent. In order to increase the available systematic data, a programme of cascade flutter investigation is at present being undertaken at N.G.T.E. This Report presents the results of tests on two types of cascade, both of 20° camber but differing in stagger angle. Preliminary results on a low stagger, 40° camber cascade have already been given.

2.0 Description of tests

2.1 Cascade details

The test cascades were each composed of 10 blades, cast in H.R. Crown Max and brazed together at the roots. Prior to assembly the individual blades had been selected to be close in their natural fundamental cantilever frequencies, in order to ensure, as nearly as possible, similar root damping characteristics. The method of assembly is shown in Figure 1(a).

Both cascades were formed of blades whose section was, in standard notation, 1004/20C50. The blade chord was 0.75 in., aspect ratio 3.0 and they were assembled with a pitch/chord ratio of 1.0. The medium stagger cascade was set at a stagger of -34.2°, while the high stagger cascade was at -44.2°.

2.2 Test techniques

These tests were carried out in the N.G.T.E. No. 6 High Speed Cascade Tunnel[1], the salient features of the working section of which are depicted in Figure 1(b). A window has been inserted in the tunnel side wall to permit the observation of the behaviour of some of the cascade blades.

The method of the optical system used to record the movements of the blade tip may briefly be described as follows. The blade under observation is fitted with a small plane stainless steel mirror of suitable diameter (in this case 0.050 in.), let into the blade tip at about 25 per cent chord from the leading edge. This mirror and a suitable area around it are illuminated by light projected by a lens from a point source. The beam reflected by the mirror comes to a focus on the film in the gate of a continuous moving film camera. As the blade vibrates, the image spot is scanned across the film at right angles to the direction of film movement, and a continuous record of the blade tip movement is thus obtained. From this can be extracted the frequency and, after suitable calibration, the alternating stress of the blade vibration. The method is also capable of recording the change in "mean" tip position, i.e., it provides a measure of the mean aerodynamic force on the blade.

The procedure for testing was to set the cascade at a fixed incidence and make film records of the blade tip movement at convenient increments of inlet air speed. Arrangements were also made to record simultaneously, by photographing manometer tubes, the total head and static pressures relevant to the aerodynamic analysis. This is essential in order to reduce the time spent in making readings at conditions of severe vibration. Even with these precautions a replacement cascade of each type was necessary to complete the ranges of incidence investigated. The limited aerodynamic analysis comprised chiefly the knowledge of the maximum and critical Mach numbers. These have been defined as follows:-

M_{nc}, the critical Mach number is that at which the pressure rise ($\Delta P/P_{tot} - P_{stat}$) first begins to fall. This will closely approximate to the drag critical Mach number usually used.

M_{nm}, the maximum Mach number is that at which the pressure rise ($\Delta P/P_{tot} - P_{stat}$) becomes zero. This is slightly below the true choking Mach number.

3.0 Test results

Both cascades were tested over a wide range of incidence and Mach number. Increments of tunnel setting angle of 1° were employed and flutter and aerodynamic recordings were made at suitable Mach numbers, (between 10 and 20 conditions per tunnel setting angle being necessary). The incidence range covered for the medium stagger cascade tests was from -11° to +20° approximately. Owing to the cascade tunnel geometry, it was impracticable to test over quite such a large range for the high stagger cascade, the actual range covered being from -11° to +14° approximately.

Flutter of the cascade blades was observed over wide ranges of incidence and was most severe at Mach numbers above the critical Mach number, M_{nc}. Whilst the majority of the vibration was of the fundamental (1st) cantilever mode, there was detected a certain amount of 2nd cantilever vibration (Figure 2) which, in the case of the medium stagger cascade, reached stresses exceeding ± 10 tons/in.^{2}.

As the record examples in Figure 2 indicate, the flutter is not always steady (comparatively speaking) but is often sporadic in character. In the analysis of the stress amplitude records, which are of 2 or 3 seconds duration for each condition, the maximum value of the alternating stress is noted together with a visual estimation of the mean alternating stress. In the case of the higher mode flutter, the stresses quoted are those near the leading edge of the nodal line nearest the blade tip (Figure 2). The alternating stresses at this point are, however, shown by calibration experiments under forced excitation conditions in the same higher mode, to be only some 10 per cent greater than the alternating stresses at the root. Consequently the root stresses in the 2nd cantilever mode can be taken as roughly the same as those plotted and, where they occur at the same time as the fundamental mode stresses, the individual stresses can arithmetically be added to obtain an estimate of the total alternating stress at the root.

3.1 Medium stagger cascade

This cascade is, in standard notation, 1004/20050 and has a stagger of -34.2°. The original cascade, used for the majority of the testing, was composed of blades whose fundamental cantilever frequencies ranged from 339 to 343 c.p.s. The replacement cascade had blades whose frequencies were in the range 325 to 350 c.p.s. approximately. An average value of the logarithmic decrement in free air was 0.007. The tip clearance used for the tests was 0.050 in.

3.1.1 Blade stresses

Figure 3 shows some typical plots of maximum alternating stress against Mach number for given inlet air angles. The maximum stress in the

fundamental cantilever mode is ±20.2 tons/in.^{2} and occurs at an air inlet angle of 64.3° (i.e. at an incidence of +20°), while the maximum stress in the 2nd cantilever mode is ±12 tons/in.^{2} at 41.1° air inlet angle, (the curve for this not being plotted in Figure 3). It will be noted that in general the curves of stress show peaks of height and width increasing with increasing inlet angle. The location of these peaks appears to be somewhat random as plotted in Figure 3. If, however, we plot the recorded stresses as contours on a base of inlet Mach number and air angle, as in Figure 4, a clearer view of the test results emerges. Plotted also in Figure 4 are the curves of critical Mach number and maximum Mach number, as evaluated from measurements made during the flutter tests, i.e. they are the oscillatory aerodynamic characteristics.

Three main regions of flutter can be distinguished in Figure 4. Firstly there is the large area above the critical Mach number curve as plotted, and extending from about 54° air inlet angle upwards as far as the test incidence range continues. This is the stalling flutter region, (the theoretical stalling air inlet angle being 53°). The second region is mainly above the maximum Mach number curve, extending over almost the complete range tested and tending to become merged with the stalling flutter region at high incidence. This is the choking flutter region. The small area of flutter just above the critical Mach number and zero incidence (which is linked to the choking flutter area) can be considered as forming a third region. This region lies in the shock-stalled part of the characteristic, and so the flutter occurring here can be termed shock-stalling flutter.

For this cascade the low incidence choking flutter occurs chiefly as 2nd cantilever vibration of moderately high stress. From about zero incidence upwards, choking flutter of the fundamental cantilever mode appears and predominates at higher incidence. The shock-stalling flutter is composed of both 1st and 2nd cantilever vibration which, over the small area where they occur simultaneously, produce stresses in excess of ±12 tons/in.^{2}. The stalling flutter is predominantly of 1st cantilever order and is extremely severe. It should here be mentioned that the identification of the 2nd cantilever mode was carried out by examining the modes of vibration of a similar isolated blade, as excited by an electromagnetic vibrator, which has frequencies close to the recorded frequency. Confirmation was obtained by a stroboscopic examination of the tip of the cascade blade when vibrating suitably in the tunnel.

3.1.2 Aerodynamic forces

As indicated in Section 2.2, a measure of the mean aerodynamic force on the vibrating blade can be made. Typical results of such measurements are given in Figure 5, in which the mean aerodynamic blade force divided by its maximum value (for a given incidence or Mach number) is plotted both against Mach number and against air inlet angle. If F is the aerodynamic force acting on the blade then the ordinates of the curves of Figure 5 are proportional to F. Comparison of Figures 4 and 5 suggests certain relationships between the experimentally plotted flutter regions and the slope of the experimentally determined force curves.

(1) Choking flutter and shock-stalling flutter coincide almost precisely with those regions in which the slope of the force versus Mach number curve is negative, i.e. where $\partial F/\partial M_n < 0$.

(2) Stalling flutter occurs, to a close approximation, with negative slope of the force versus incidence curve, i.e. where $\partial F/\partial \alpha_1 < 0$.

It will be noted however that $\partial F/\partial \alpha_1$ becomes positive again at α_1 = 61° approximately, this being accompanied by an increase in the recorded flutter stresses! The mechanism of the flutter in this region is not apparent, but may well be due to a hysteresis loop effect in the lift curve (starting from α_1 = 61°) similar to the stall point hysteresis effect described, for example, in Reference 2. A general outline of the areas of negative slope of $\partial F/\partial M_n$ and $\partial F/\partial \alpha_1$ is shown in Figure 6(a), the regions of flutter greater than ±5 tons/in.^{2} being shown also for comparison purposes. It is seen that the criterion of negative $\partial F/\partial M_n$ and $\partial F/\partial \alpha_1$, for flutter, holds to a good approximation.

3.2 High stagger cascade

This cascade, of form 1004/20050 and stagger -44.2° was tested with a tip clearance of 0.050 in. The blades' fundamental cantilever frequencies ranged from 334 to 341 c.p.s. for the original cascade, whilst those of the replacement cascade lay between 366 and 377 c.p.s. The average logarithmic decrement in free air was 0.004.

3.2.1 Blade stresses

Typical plots of maximum alternating stress against inlet Mach number are given in Figure 7, from which it will be seen that most of the stress peaks appear to lie in the Mach number range 0.7 to 0.9, with additional high stresses at the upper end of the Mach number range. The maximum fundamental cantilever stress reached is ±22.4 tons/in.^{2} at the maximum air inlet angle tested, viz. 67.8° (i.e. at an incidence of +14°). It will also be noted that flutter in the 2nd cantilever mode is again present (as with the medium stagger cascade) but at much reduced stresses, not exceeding ±3 tons/in.^{2}. In Figure 8 are plotted the complete range of test results as stress levels on a base of inlet angle and inlet Mach number, together with the oscillatory aerodynamic characteristics, M_{nm} and M_{nc}. On examination of Figure 8, two of the major flutter regions are apparent, viz, choking flutter, mainly above the maximum Mach number curve, and stalling flutter, from about 56° inlet angle onwards. There is apparently no distinct region attributable to shock-stalling flutter. It should also be noted that severe stalling flutter extends to a certain extent below the critical Mach number whereas, in the case of the medium stagger cascade, no severe flutter appeared below the critical Mach number.

3.2.2 Aerodynamic forces

Some of the results of the measurements of the mean blade tip displacement, to which the mean aerodynamic blade force is proportional, are plotted in Figure 9. It is noted that while for the choking flutter regions $\partial F/\partial M_n$ is negative, the lag of the onset of choking flutter on the beginning of the region of negative $\partial l/\partial M_n$ is greater than is the case with the medium stagger cascade (Figure 5).

The curve of Figure 9(b) shows that the derivative $\partial F/\partial \alpha_1$, as measured under oscillatory conditions, first becomes negative almost precisely with the onset of stalling flutter, although within 5 degrees it becomes sharply positive and then negative again. This second peak of blade force is very close to the theoretical stalling inlet angle (62°), but the doubtful accuracy of stalling incidence predictions may reduce the significance of this. The suggestion of a short range of negative $\partial F/\partial M_n$ on the force curve for α_1 = 57.3°, Figure 9(a), together with the appearance of the mean stress contour diagram, Figure 8(b), might be taken to indicate that the flutter from about 56.6° → 58° is in fact

shock-stalling flutter. The shape of the force v. incidence curve of Figure 9(b) is, however, repeated for other values of Mach number both within and without the flutter range, thus showing that the incidence stall at 56.5° is a true incidence stall, and not one induced by the proximity of another flutter zone. Unfortunately the force curves for inlet angles close to 57.3° have a scarcity of points in the M_n range 0.7 to 0.8 and so it is impossible to verify the short range negative $\partial F/\partial M_n$ of 57.3°. It can only be said, then, that while the blade exhibits stalling flutter from 56° inlet angle upwards, there is the possibility that it also shows shock-stalling flutter during the initial part of the stalling flutter region.

The general disposition of regions of negative $\partial F/\partial M_n$ and $\partial F/\partial \alpha_1$ and their location relative to regions of stress greater than $\pm$ 5 tons/in.^{2} will be noted in Figure 6(b). As was mentioned above, the region of negative $\partial F/\partial M_n$ starts at a lower Mach number compared with the onset of choking flutter than is the case with the medium stagger cascade.

4.0 Theoretical aspects

Although the forces acting on a blade when stalled are very complex and almost impossible to calculate, it is, however, instructive to make a simplified approach to the problem, in the hope of revealing the mechanism of the flutter.

It is assumed that the force F on the blade at any instant is a function of the instantaneous inlet air velocity $V_1 + \Delta V_1$ and inlet angle $\alpha_1 + \Delta\alpha_1$. By constructing the velocity triangles for the system of a blade, vibrating at right angles to its chord, in an incident airstream, and by neglecting any aerodynamic lag in the flow vectors, the following expressions for the instantaneous inlet velocity and angle are obtained.

$$V_1 + \Delta V_1 = V_1 - \dot{x} \sin(\alpha_1 - |\zeta|) \quad \ldots\ldots\ldots\ldots\ldots\ldots\ldots\ldots\ldots\ldots(1)$$

$$\alpha_1 + \Delta\alpha_1 = \alpha_1 - \frac{\dot{x}}{V_1} \cos(\alpha_1 - |\zeta|) \quad \ldots\ldots\ldots\ldots\ldots\ldots\ldots\ldots\ldots\ldots(2)$$

where $\dot{x}$ = instantaneous blade velocity

$= \dot{x}_o \cos \omega t$

$\dot{x}_o$ = maximum blade velocity

ω = angular frequency of blade vibration

ζ = blade stagger

Therefore the expression for the work done on the blade by the incident airstream per cycle can be expanded as follows:-

$$\int_0^{\frac{2\pi}{\omega}} F(V_1 + \Delta V_1, \alpha_1 + \Delta\alpha_1)\, \dot{x}\, dt$$

$$\doteq \int_0^{\frac{2\pi}{\omega}} \left\{ F(V_1, \alpha_1) + \Delta V_1 \frac{\partial F}{\partial V_1} + \Delta\alpha_1 \frac{\partial F}{\partial \alpha_1} \right\} \dot{x}\, dt$$

$$= \frac{\pi \dot{x}_o^2}{\omega V_C} \left\{ - \frac{\partial F}{\partial M_n} \cdot \sin(\alpha_1 - |\zeta|) - \frac{\partial F}{\partial \alpha_1} \cdot \frac{\cos(\alpha_1 - |\zeta|)}{M_n} \right\} \quad \ldots(3)$$

where V_C = the acoustic velocity.

When the work done on the blade per cycle is positive, (neglecting the effect of damping), the vibration is self-induced, i.e. blade flutter occurs. From expression (3) it is seen that, according to the simple theory applied, the prediction of flutter becomes a study of the derivatives $\partial F/\partial M_n$ and $\partial F/\partial \alpha_1$, flutter occurring when either or both derivatives have certain negative values. Sections 3.1.2 and 3.2.2 have shown that the correlation both between negative $\partial F/\partial M_n$ and choking and shock-stalling flutter, and between negative $\partial F/\partial \alpha_1$ and stalling flutter, is good, the values of the derivatives being measured under oscillatory conditions.

It will be noted from expression (3) that the relative contribution of negative $\partial F/\partial M_n$ and negative $\partial F/\partial \alpha_1$ to flutter is controlled by $\alpha_1 - |\zeta|$. Due in part to the inaccuracy of assessing the large negative values of $\partial F/\partial M_n$ that occur, as well as to the inadequacy of the simple theory, the insertion of the experimentally derived values of $\partial F/\partial M_n$ and $\partial F/\partial \alpha_1$ in expression (3) leads to a certain amount of discrepancy in the correlation of points of positive value of (3) and flutter. For example, having plotted out the results of the medium stagger cascade tests in a form suitable for the application of (3), it was seen that there was reasonable correlation for stalling flutter, near-correlation for some of the 1st cantilever choking flutter, but no correlation for the negative incidence, 2nd cantilever choking flutter. This last discrepancy can, in part, be explained by the fact that the expression (3) is based on the assumption of blade movement at right angles to blade chord, to which condition 1st cantilever vibration closely approximates, but from which the 2nd cantilever mode considerably differs.

5.0 Discussion of results

The main conclusions to emerge from these tests are that flutter of considerable magnitude occurs with both the medium and high stagger cascades, and that three types of flutter, similarly disposed with reference to the aerodynamic characteristics, can be distinguished.

(1) Stalling flutter

This type occurs at incidences above stall and is of considerable extent. The force derivative $\partial F/\partial \alpha_1$ is mainly negative in this region.

(2) Shock-stalling flutter

This occurs at or just above the drag critical Mach number and is usually confined to narrow limits of M_n and α_1, the incidence being low. The force derivative $\partial F/\partial M_n$ is negative.

(3) Choking flutter

This occurs when the cascade is choked and extends over quite a wide range of incidence, $\partial F/\partial M_n$ being negative.

Whilst the shock-stalling flutter is quite distinct in the case of the medium stagger cascade, it is thought that for the high stagger cascade it is present within a small part of the stalling flutter region. It is interesting to note that the small "pocket" of 2nd cantilever vibration at about 55° for the medium stagger cascade (Figure 4), which comes within the category of shock-stalling flutter (see Figure 5,), is also very close to and partly overlaps the stalling flutter region.

The apparent lower Mach number limit to stalling flutter as shown in Figures 4 and 8, despite the fact that the region of negative $\partial F/\partial a_1$ is not similarly limited (Figure 6), might be taken to indicate that the "working line" of a compressor stage could be designed to pass, at high incidences, into a flutter - immune area (at low Mach number). That this is not the case however is apparent upon examination of Figures 3 and 7, from which it is seen that even at very low Mach numbers there is still stalling flutter of appreciable stress.

Although flutter occurs at high stresses (up to ±12 tons/in.^{2}) in the 2nd cantilever mode on the medium stagger cascade, it occurs only at low stresses for the high stagger cascade. In both cascades however, stalling flutter is predominantly of the fundamental cantilever mode and is of very high stress. The maximum stresses occurring with all three types of flutter are of sufficient magnitude to cause blade failures within a very short time. Choking and stalling conditions can be obtained, under certain operating conditions, in compressors. In particular it is difficult to see, from these results, how stalling flutter conditions can be avoided in a high duty compressor, operating over a wide speed range. In addition, the shock-stalling flutter region is not very far removed from the nominal design point of many compressor stages and it is possible that in certain circumstances e.g. at overspeed, some sections of the blades might be working in that zone.

The correlation of flutter zones with the negative values of the oscillatory force coefficients $\partial F/\partial M_n$ and $\partial F/\partial a_1$ has been shown to be good, though better for the medium stagger than for the high stagger cascade (Figure 6). The comprehensive flutter criterion, deduced in Section 4 from simple assumptions, is seen to give good correlation for stalling flutter only. At this stage therefore, it would appear that it is more realistic to use the individual behaviour of the experimental (oscillatory) values of the force coefficients as flutter criterions, negative $\partial F/\partial a_1$ for stalling flutter and negative $\partial F/\partial M_n$ for choking and shock-stalling flutter.

It should be emphasised that the results here presented derived from cascade tests on blades of constant thickness/chord ratio and aspect ratio, and with similar material and root damping properties. The characteristics thus evinced take no account of the effect of these parameters. It is felt however that the flutter aspects presented for these low camber cascades are of a fairly general nature.

6.0 Conclusions

This Report presents the results of the first part (viz. medium and high stagger, low camber cascades) of the present programme of

cascade flutter investigation being pursued at N.G.T.E. Three main types of flutter, stalling, shock-stalling and choking flutter are shown to occur at stresses sufficiently high to cause early blade failure.

The study of the experimentally obtained blade force derivatives (with respect to M_n and α_1) is shown to give good flutter prediction. More experimental data however, are required before the work can be put on a quantitative basis.

REFERENCES

No.	Author(s)	Title
1	A. D. S. Carter	Some Tests on Compressor Cascades of Related Aerofoils having Different Positions of Maximum Camber. December, 1948. R. & M. 2694.
2	M. Victory	Flutter at High Incidence. R. & M. 2048. January, 1943.

FIG. 1

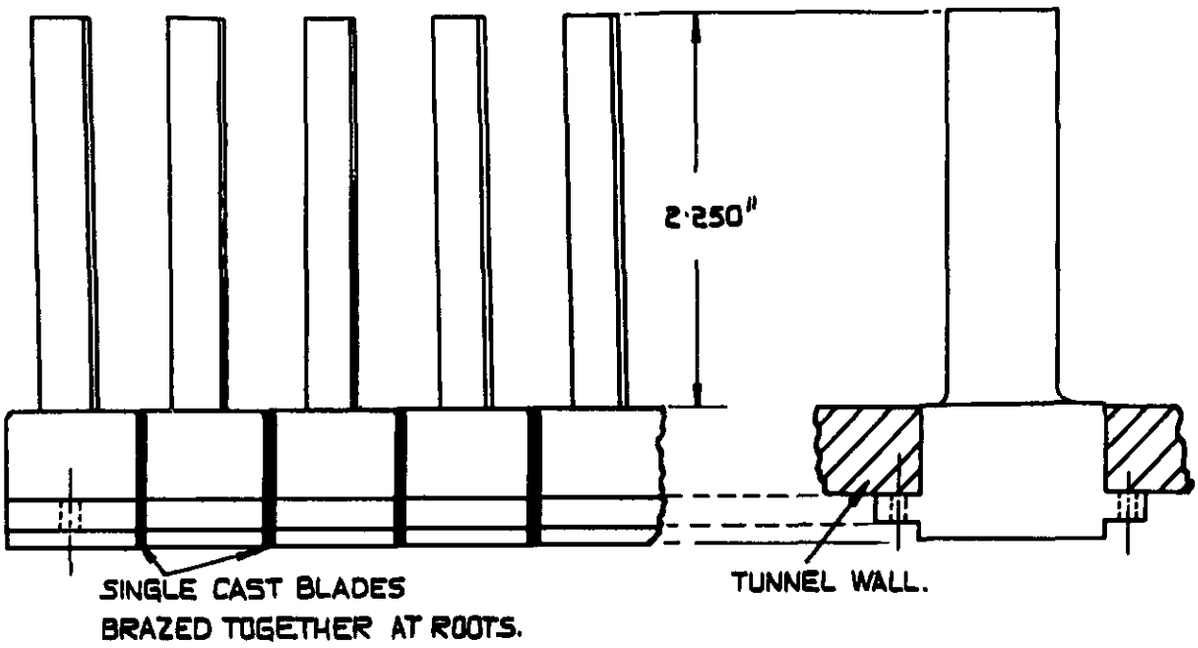

(a) ROOT ATTACHMENT OF BLADES.

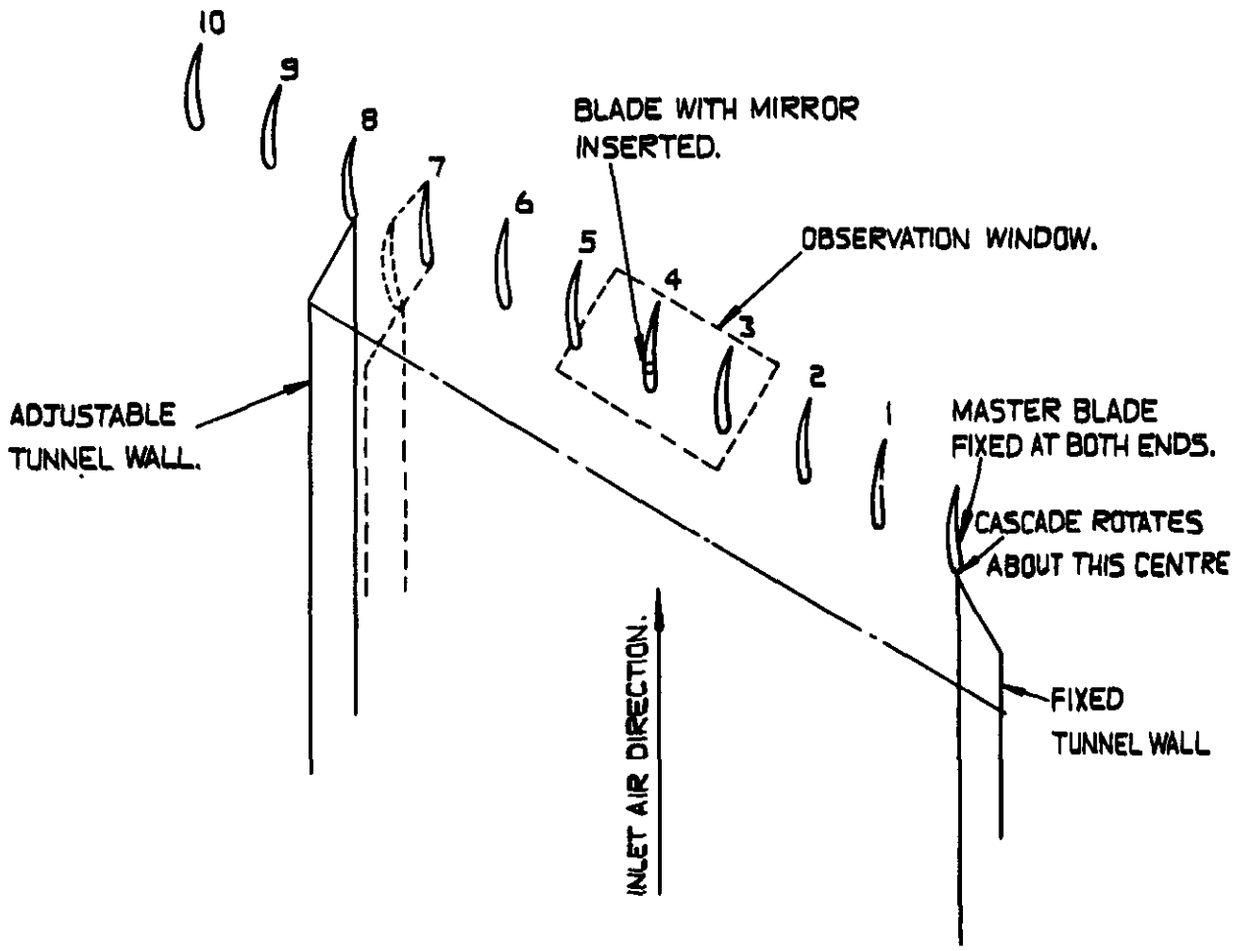

(b) LOCATION OF CASCADE IN TUNNEL.

CASCADE AND TUNNEL ARRANGEMENTS.

FIG.2

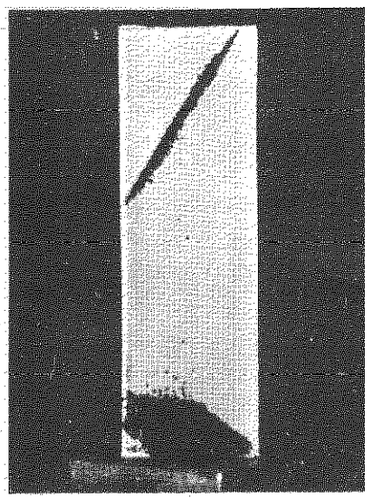

2ND CANTILEVER MODE
10C4 / 20C50, $\zeta = -34.2°$

(a) CASCADE BLADE NODAL PATTERN

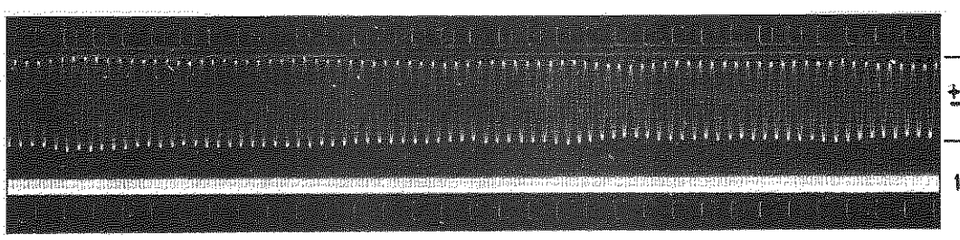

FUNDAMENTAL CANTILEVER MODE, 337 c.p.s., $M_h = 0.69$, $\alpha_1 = 56.4°$
10C4/20C50, $\zeta = -44.2°$

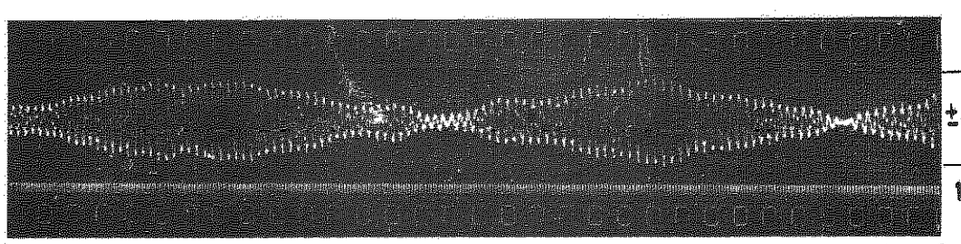

FUNDAMENTAL CANTILEVER MODE, 340 c.p.s., $M_h = 0.65$, $\alpha_1 = 59.8°$

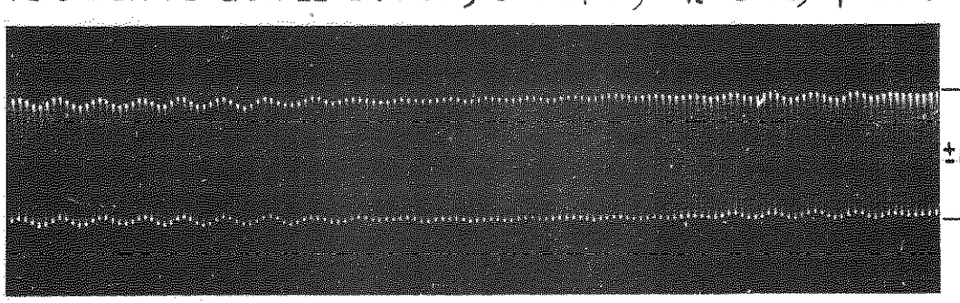

(x 2 ENLARGEMENT, FILM SPEED 48 INS. PER SEC.)
2ND CANTILEVER MODE, 2110 c.p.s., $M_h = 0.97$, $\alpha_1 = 44.4°$
10C4 / 20C50, $\zeta = -34.2°$

(b) TYPICAL FLUTTER RECORDS.

NODAL PATTERN AND FLUTTER RECORDS.

FIG 3

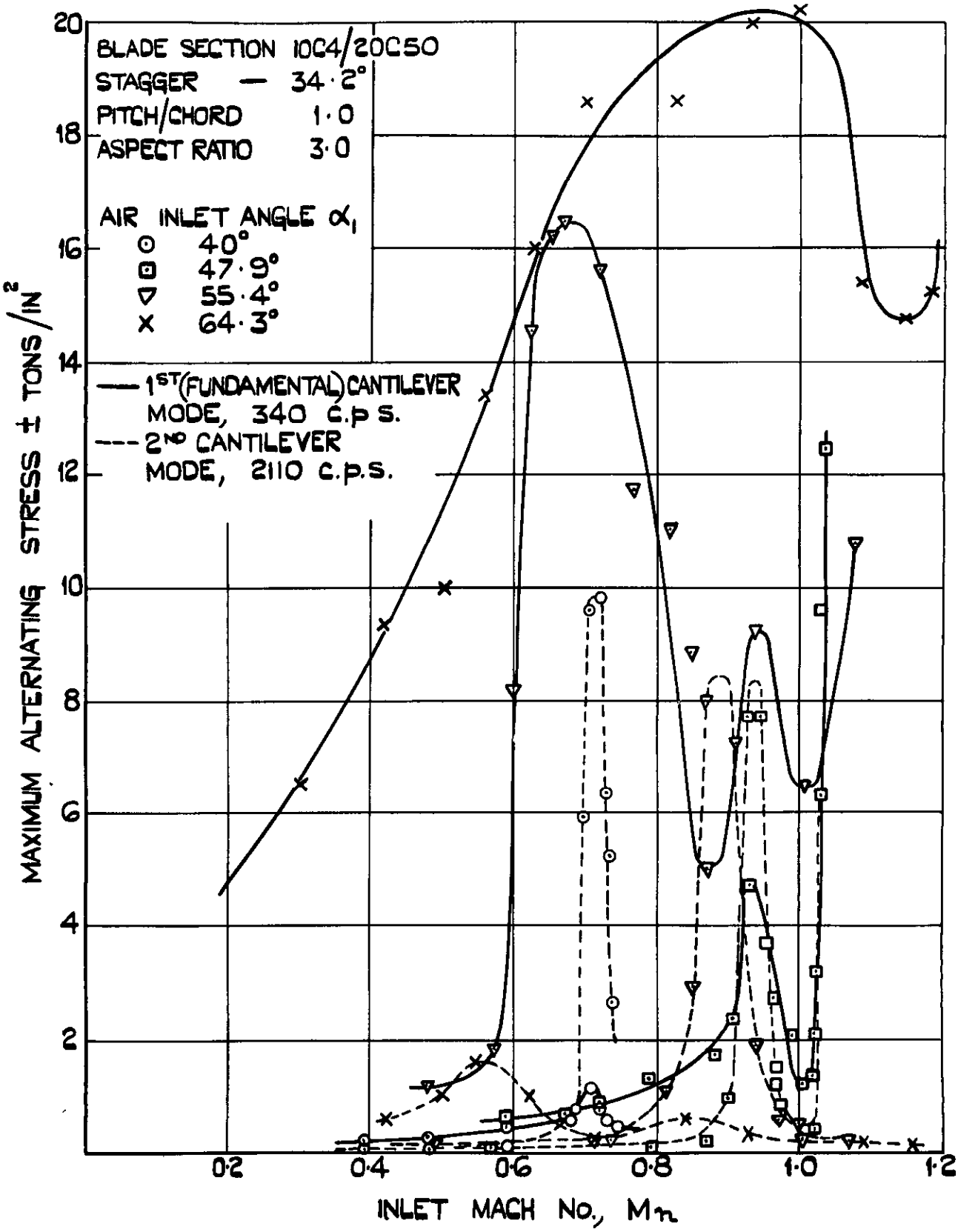

FLUTTER CHARACTERISTICS FOR MEDIUM STAGGER CASCADE

FIG.4

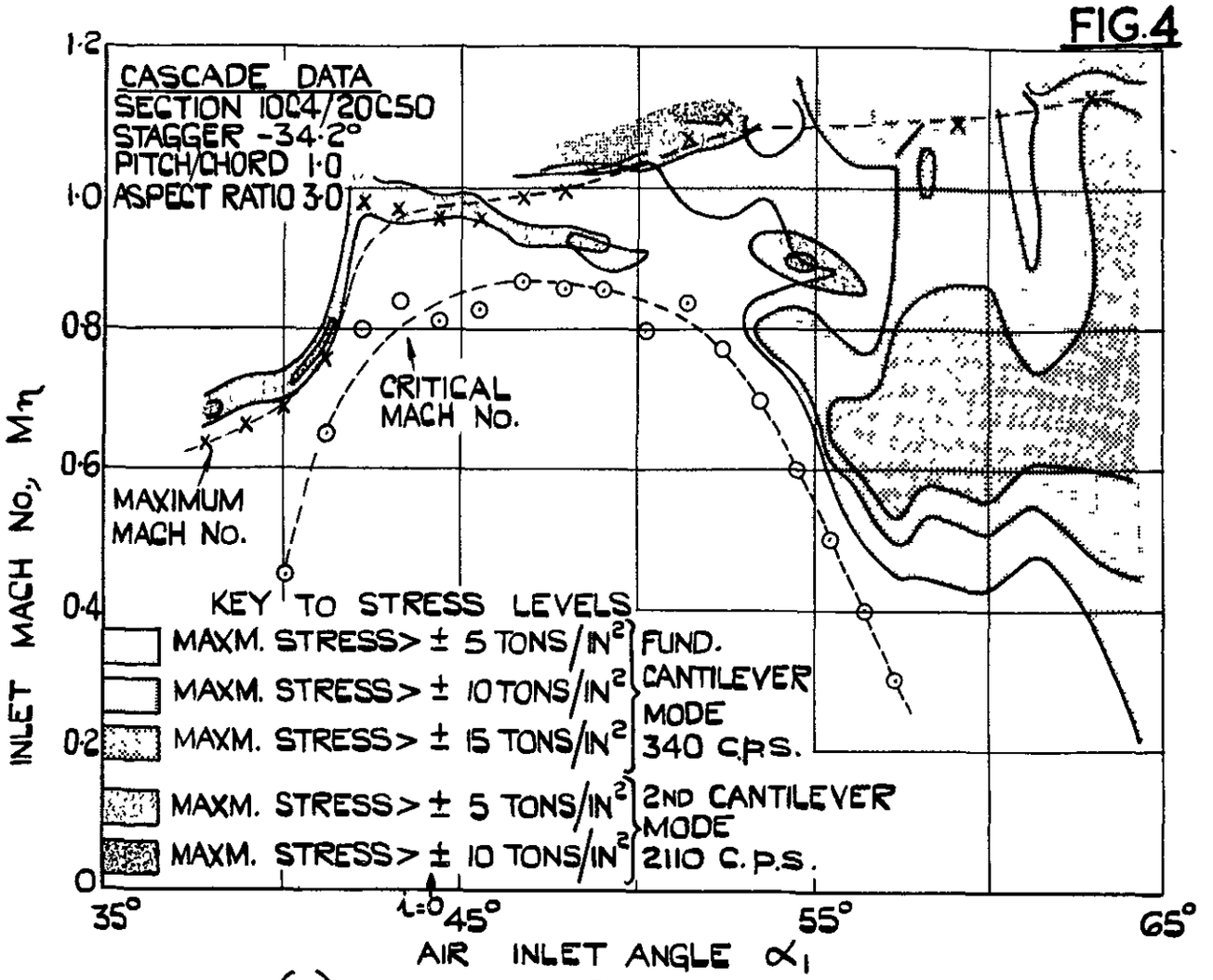

(a) MAXIMUM STRESS LEVELS

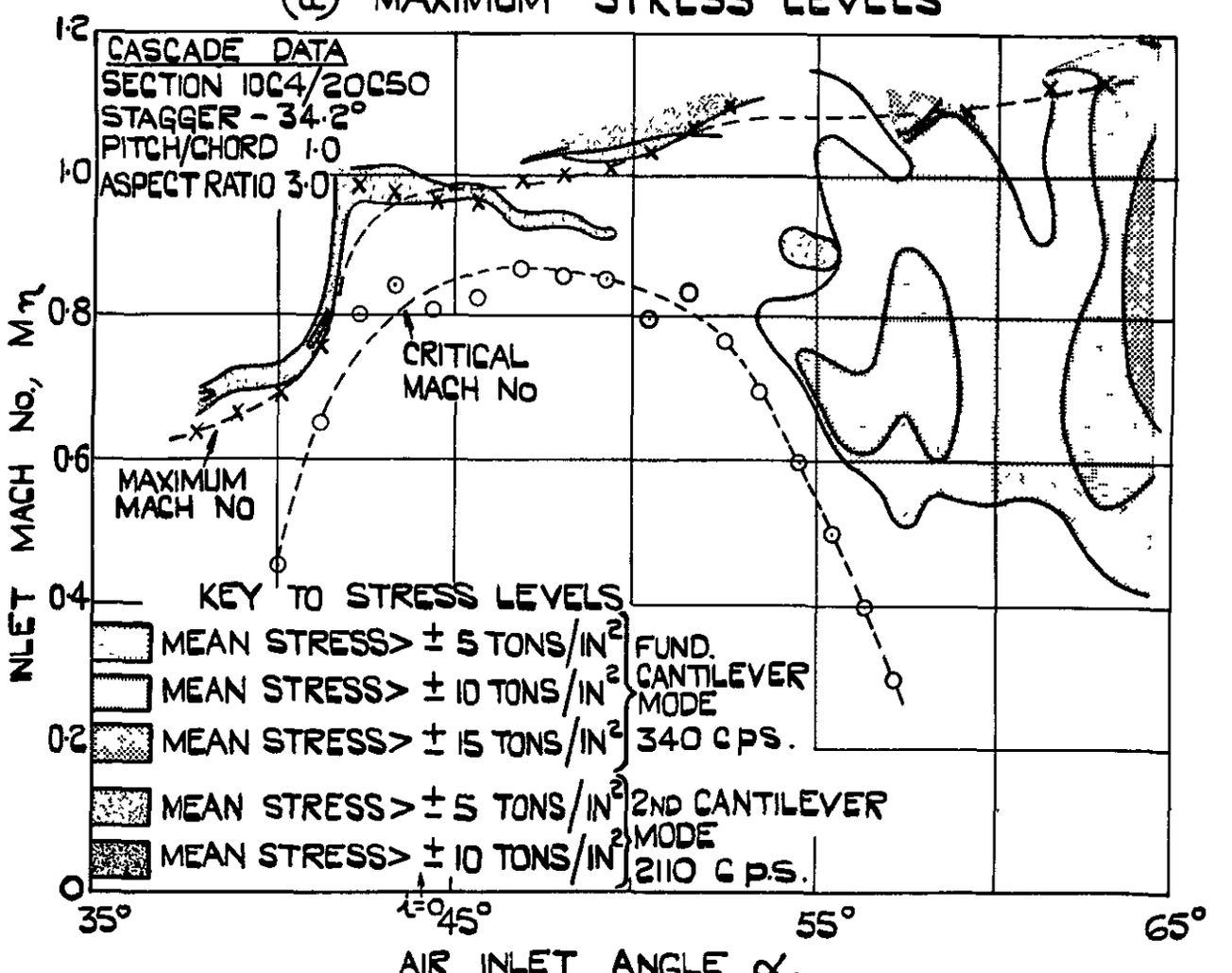

(b) MEAN STRESS LEVELS

LOCATION OF FLUTTER (MEDIUM STAGGER CASCADE)

FIG.5

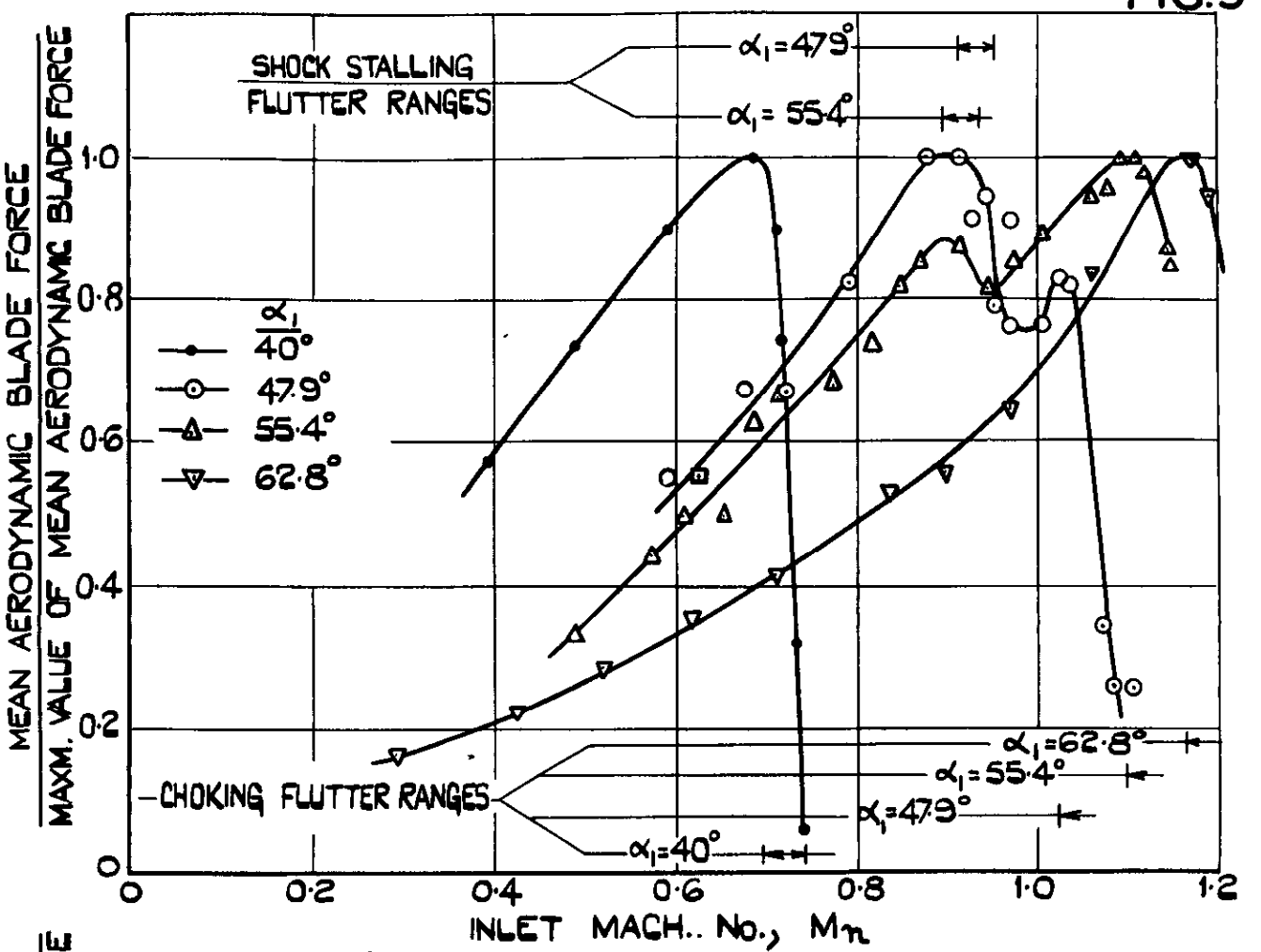

(a) FORCE V MACH. No.

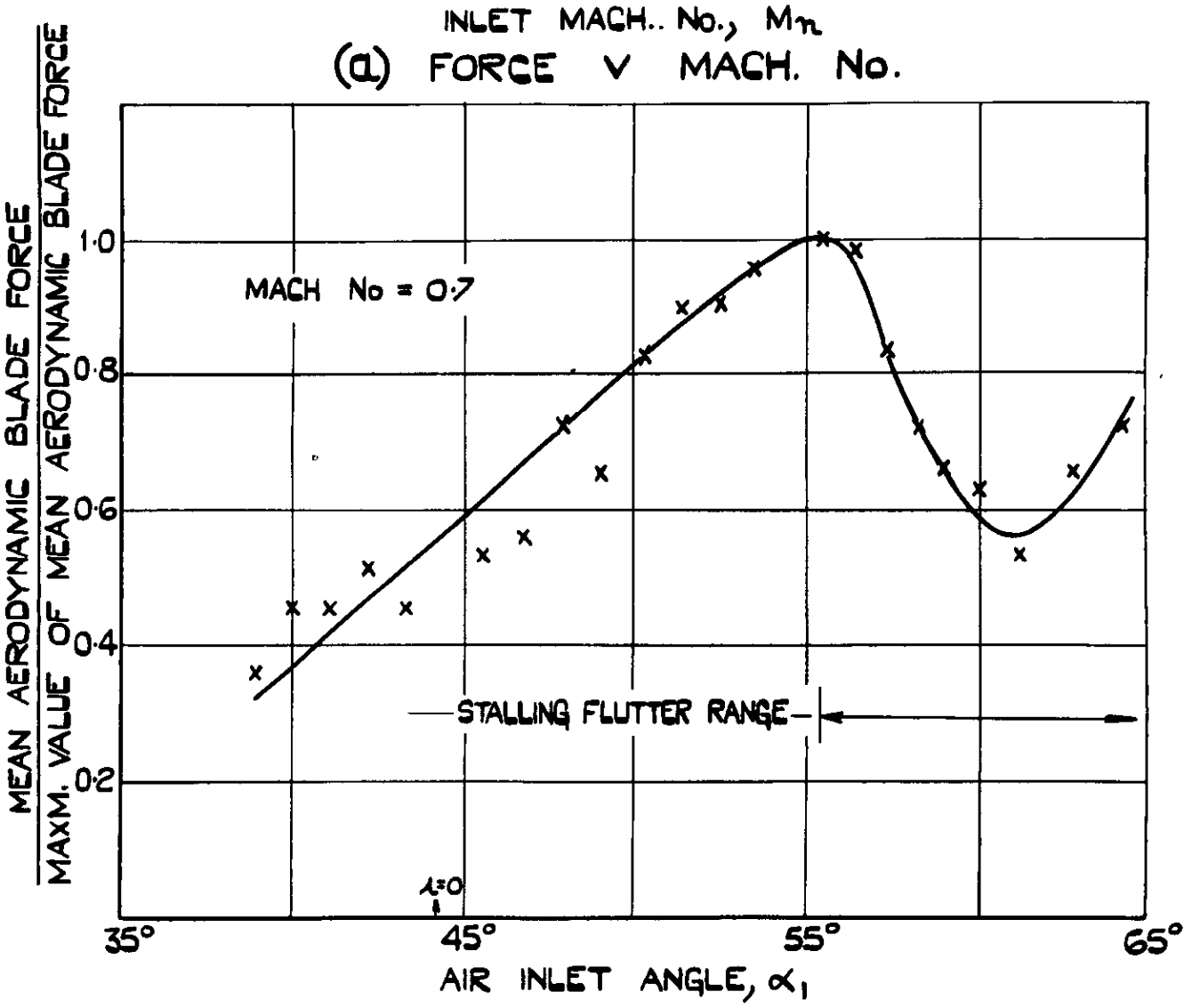

(b) FORCE V INCIDENCE.

NOTE :- FORCE MEASUREMENTS MADE ON VIBRATING BLADE

FORCE CHARACTERISTICS FOR MEDIUM STAGGER CASCADE BLADE.

FIG.6

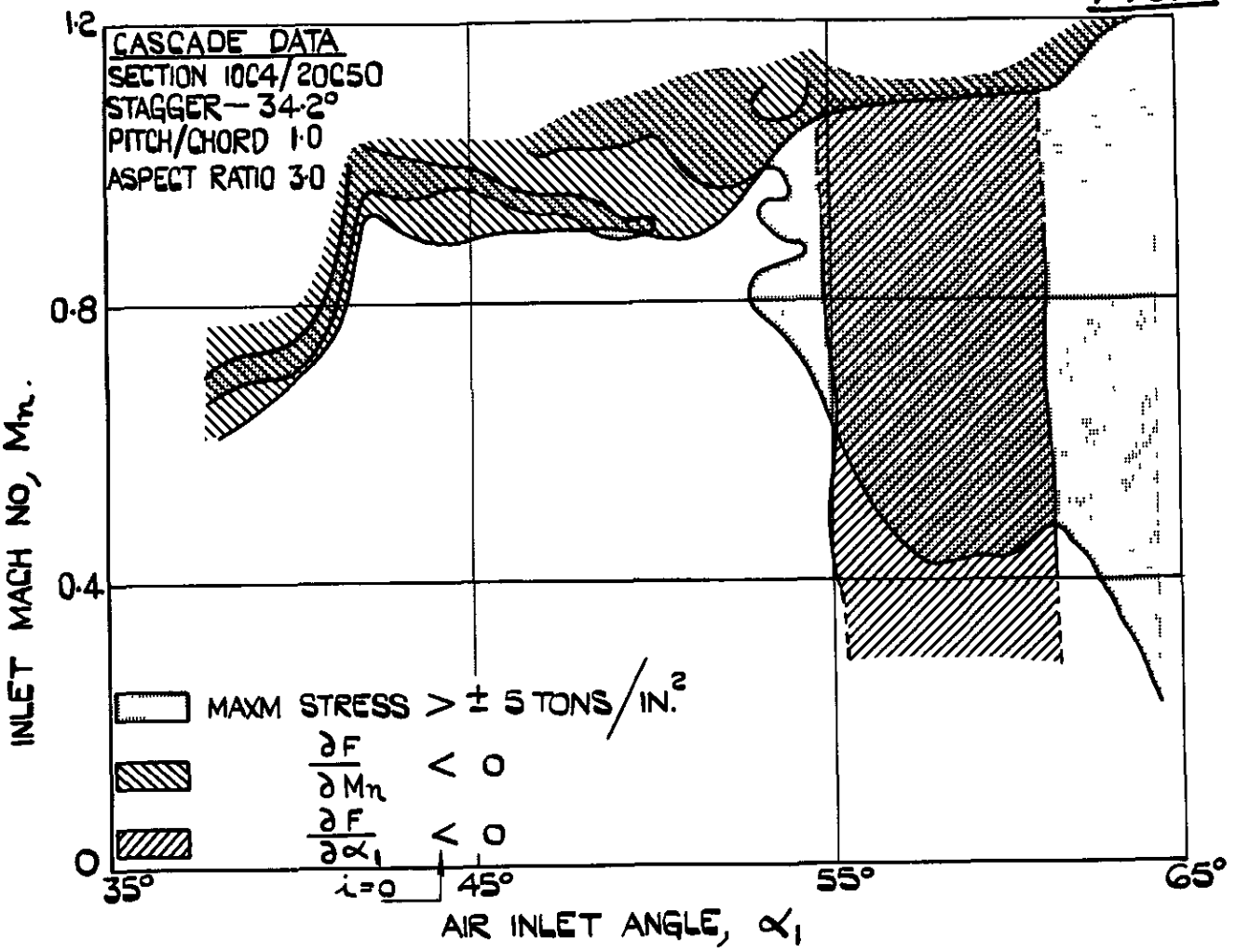

(a) MEDIUM STAGGER CASCADE

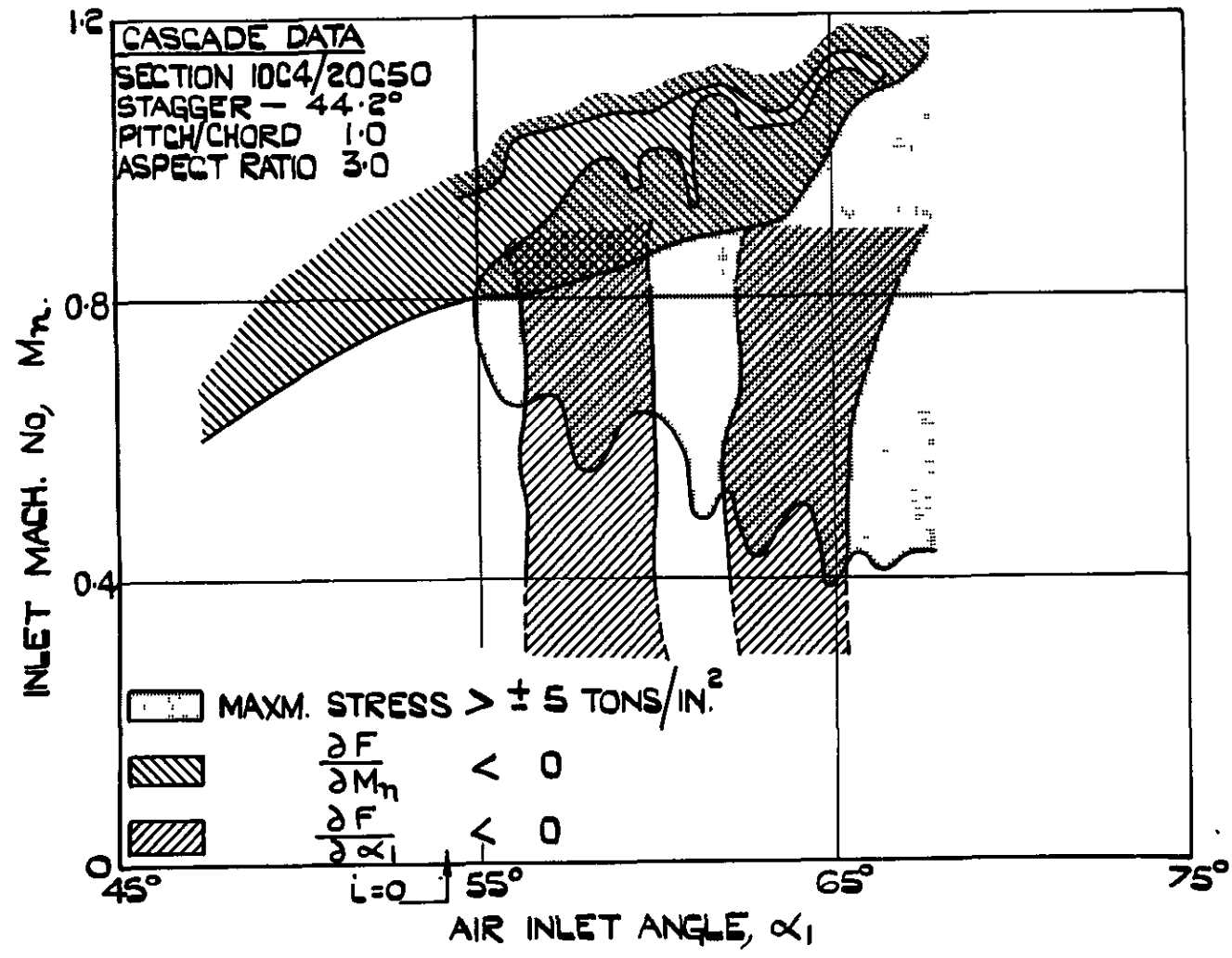

(b) HIGH STAGGER CASCADE.

COMPARISON OF REGIONS OF NEGATIVE SLOPE OF FORCE CURVES AND FLUTTER

FIG. 7

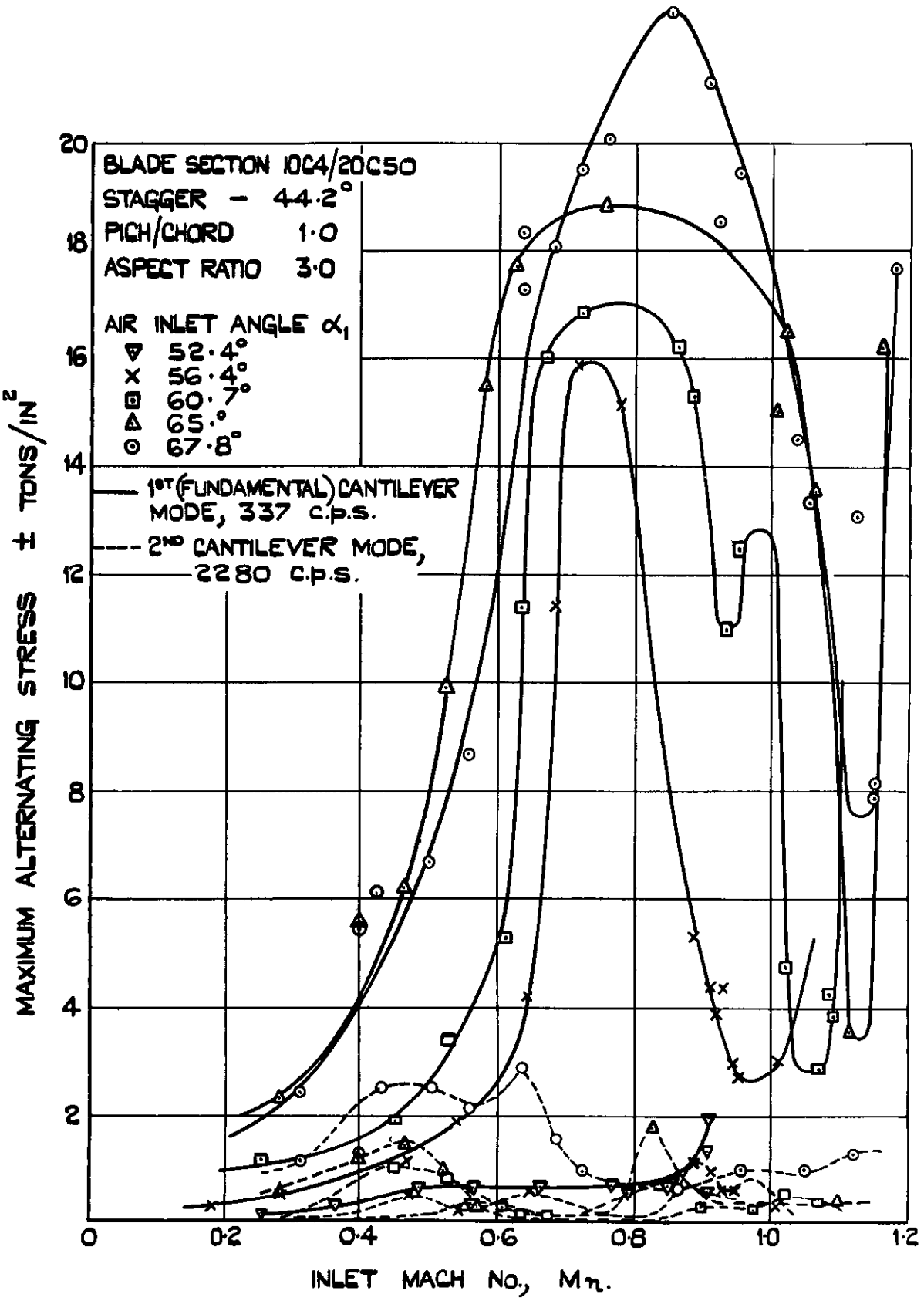

FLUTTER CHARACTERISTICS FOR HIGH STAGGER CASCADE.

FIG.8

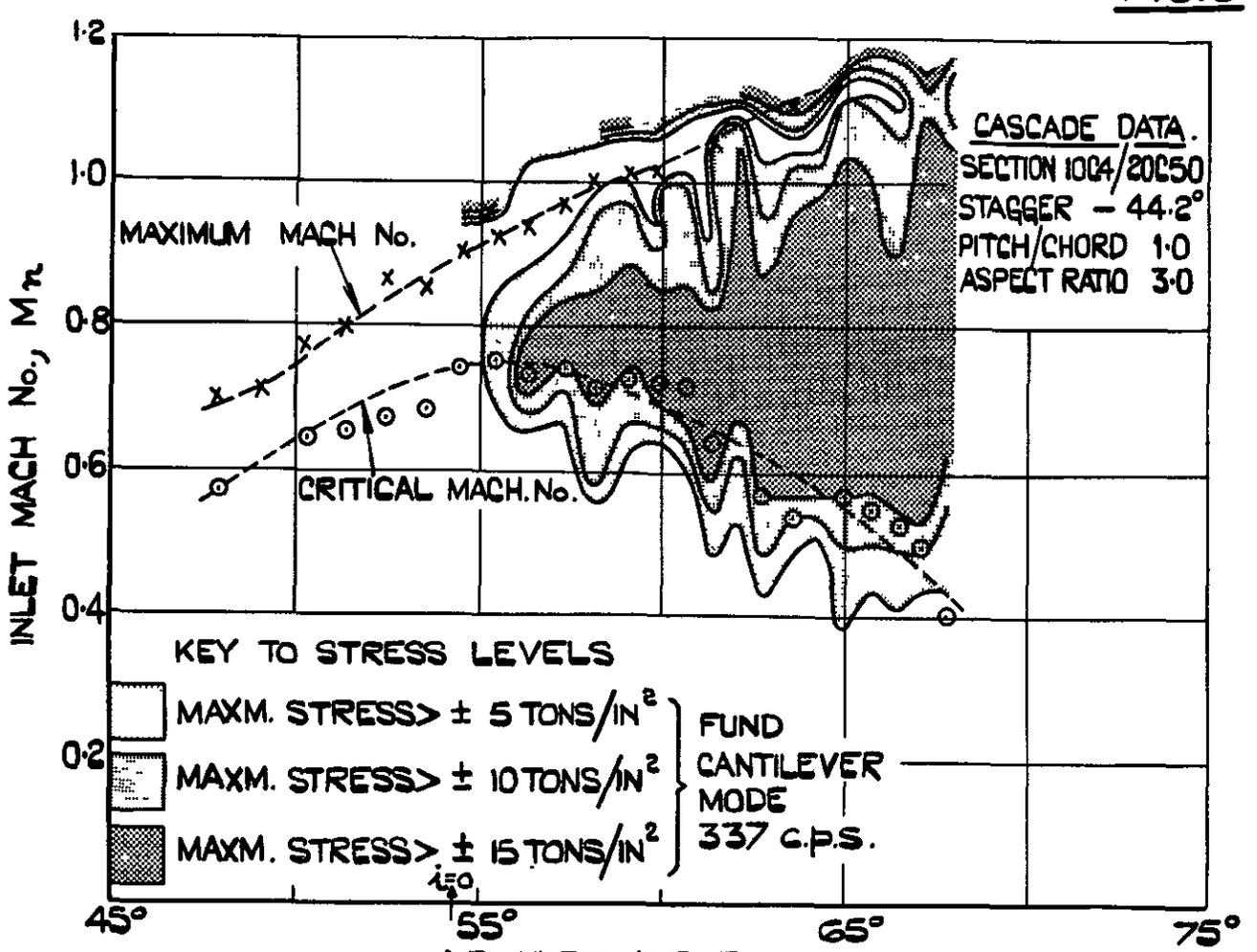

(a) MAXIMUM STRESS LEVELS.

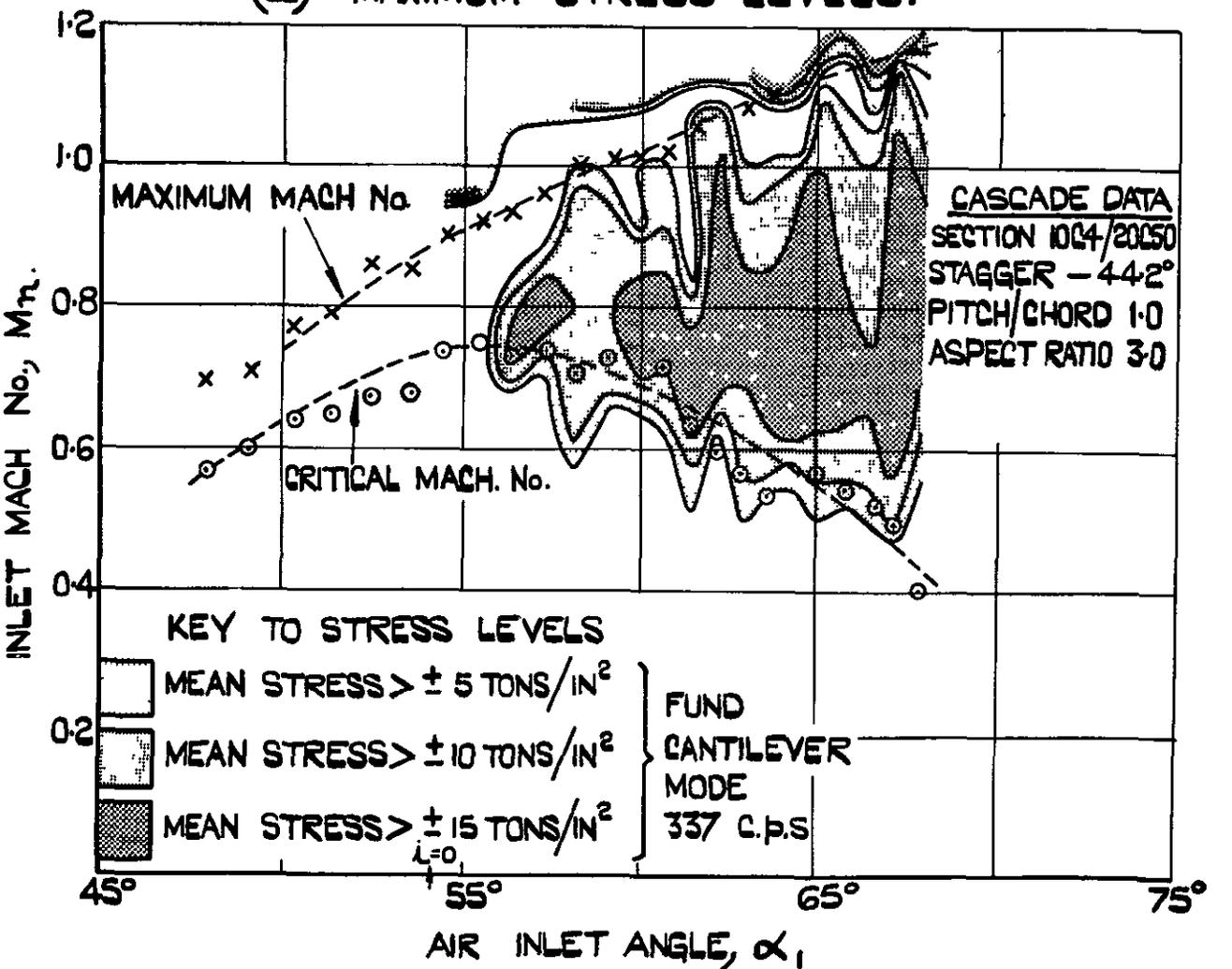

(b) MEAN STRESS LEVELS.

LOCATION OF FLUTTER (HIGH STAGGER CASCADE.)

FIG.9

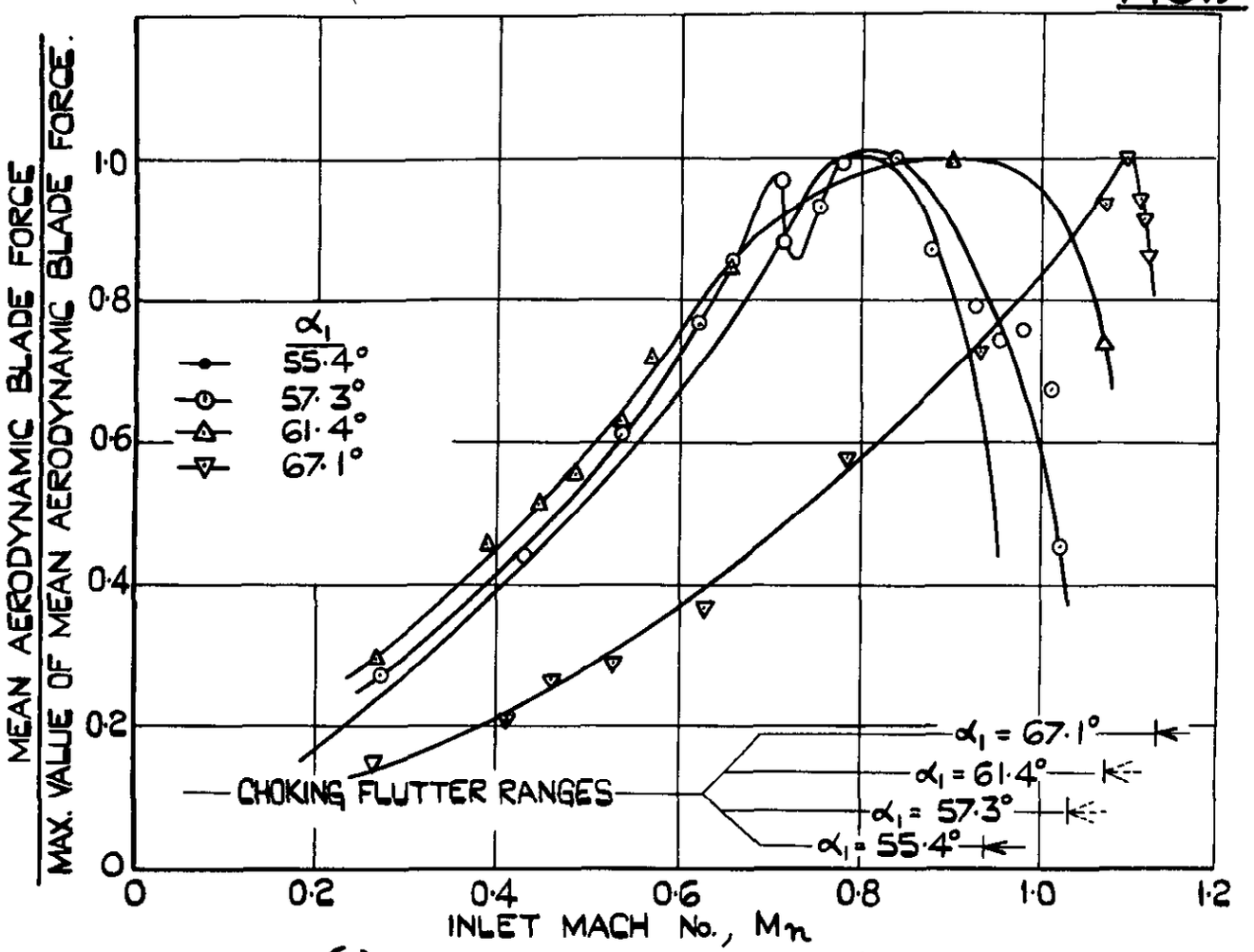

(a) FORCE V MACH. No.

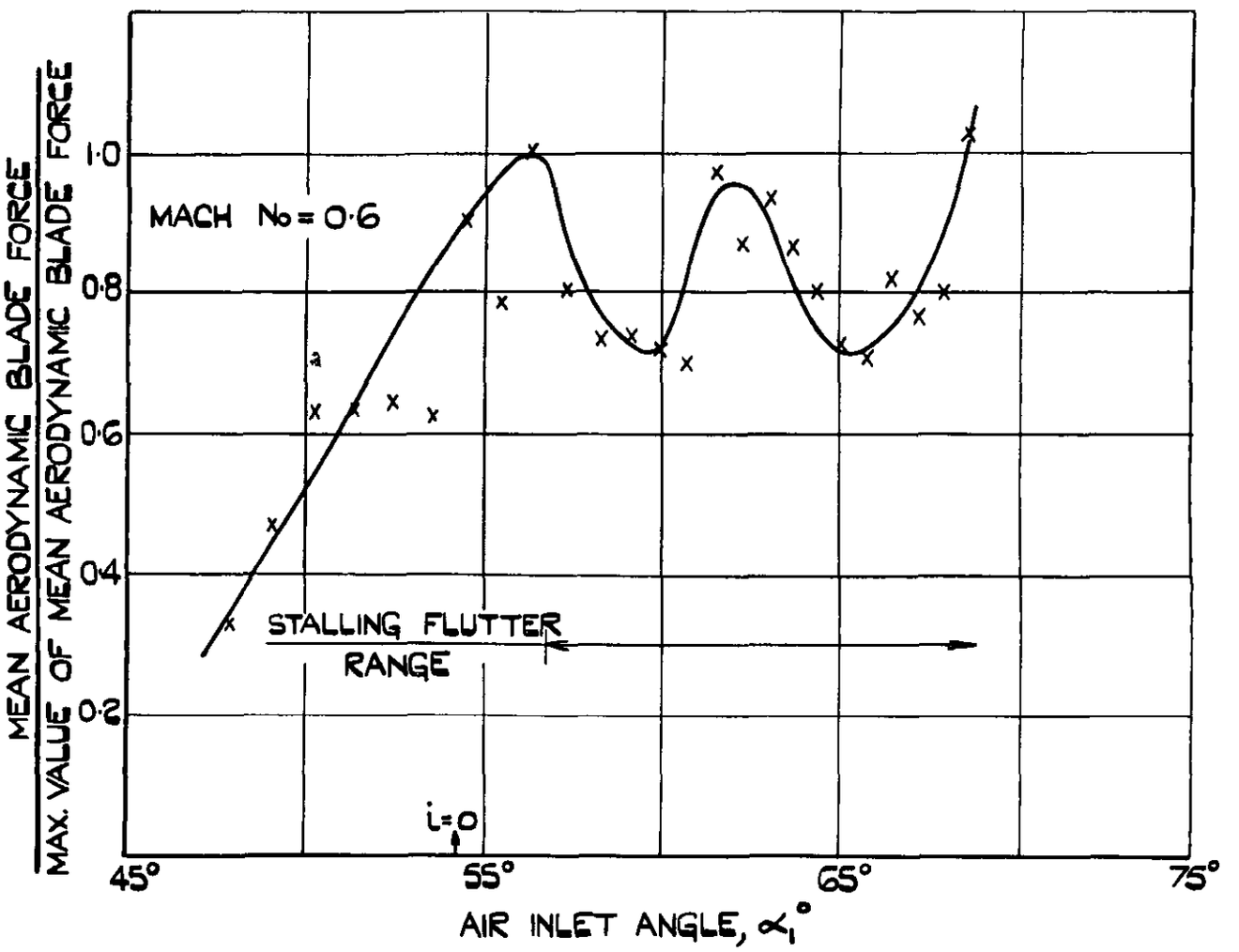

(b) FORCE V INCIDENCE

(NOTE:- FORCE MEASUREMENTS MADE ON VIBRATING BLADE)

FORCE CHARACTERISTICS FOR HIGH STAGGER CASCADE BLADE.

C.P. No. 187
(16,887)
A R C Technical Report

PRINTED AND PUBLISHED BY HER MAJESTY'S STATIONERY OFFICE
To be purchased from
York House, Kingsway, LONDON, W C 2 — 423 Oxford Street, LONDON, W 1
P O Box 569, LONDON, S E 1
13a Castle Street, EDINBURGH, 2 — 109 St Mary Street, CARDIFF
39 King Street, MANCHESTER, 2 — Tower Lane, BRISTOL, 1
2 Edmund Street, BIRMINGHAM, 3 — 80 Chichester Street, BELFAST
or from any Bookseller
1955
Price 2s 6d net
PRINTED IN GREAT BRITAIN

S O. Code No. 23-9007-87

C.P. No. 187